



**HAL**  
open science

## **A silicon nitride ISFET based immunosensor for tumor necrosis factor-alpha detection in saliva. A promising tool for heart failure monitoring**

Hamdi Ben Halima, Francesca Bellagambi, Albert Alcacer, Pfeiffer Norman, Albert Heuberger, Marie Hangouët, Nadia Zine, Joan Bausells, Abdelhamid Elaïssari, Abdelhamid Errachid

### ► To cite this version:

Hamdi Ben Halima, Francesca Bellagambi, Albert Alcacer, Pfeiffer Norman, Albert Heuberger, et al.. A silicon nitride ISFET based immunosensor for tumor necrosis factor-alpha detection in saliva. A promising tool for heart failure monitoring. *Analytica Chimica Acta*, 2021, 1161, pp.338468. 10.1016/j.aca.2021.338468 . hal-03200127

**HAL Id: hal-03200127**

**<https://hal.science/hal-03200127v1>**

Submitted on 1 Jun 2021

**HAL** is a multi-disciplinary open access archive for the deposit and dissemination of scientific research documents, whether they are published or not. The documents may come from teaching and research institutions in France or abroad, or from public or private research centers.

L'archive ouverte pluridisciplinaire **HAL**, est destinée au dépôt et à la diffusion de documents scientifiques de niveau recherche, publiés ou non, émanant des établissements d'enseignement et de recherche français ou étrangers, des laboratoires publics ou privés.

1        **A silicon nitride ISFET based immunosensor for Tumor Necrosis Factor-**  
2        **alpha detection in saliva. A promising tool for heart failure monitoring**

3        Hamdi Ben Halima<sup>a</sup>, Francesca G. Bellagambi<sup>a,\*</sup>, Albert Alcacer<sup>b</sup>, Norman Pfeiffer<sup>c</sup>, Albert  
4        Heuberger<sup>d</sup>, Marie Hangouët<sup>a</sup>, Nadia Zine<sup>a</sup>, Joan Bausells<sup>b</sup>, Abdelhamid Elaissari<sup>a</sup>,  
5        Abdelhamid Errachid<sup>a,\*</sup>

6  
7  
8        <sup>a</sup> University Claude Bernard Lyon 1, Institute of Analytical Sciences (ISA) – UMR 5280, 5 rue de la  
9        Doua, 69100, Lyon, France.

10        <sup>b</sup> Institute of Microelectronics of Barcelona (IMB–CNM, CSIC), Campus UAB, 08193 Bellaterra,  
11        Barcelona, Spain.

12        <sup>c</sup> Fraunhofer IIS, Fraunhofer Institute for Integrated Circuits, Am Wolfsmantel 33, 91058 Erlangen,  
13        Germany.

14        <sup>d</sup> Information Technology (LIKE), Friedrich-Alexander-Universität Erlangen-Nürnberg (FAU), Am  
15        Wolfsmantel 33, 91058 Erlangen, Germany.

16  
17  
18        **\* Corresponding authors**

19        *E-mail address:* [francesca.bellagambi@univ-lyon1.fr](mailto:francesca.bellagambi@univ-lyon1.fr)

20        Telephone: +33 43 74 23 569

21        ORCID iD: 0000-0002-1608-8858

22        Scopus Author iD: 55942967100

23  
24        *E-mail address:* [abdelhamid.errachid-el-salhi@univ-lyon1.fr](mailto:abdelhamid.errachid-el-salhi@univ-lyon1.fr)

25        Telephone: +33 43 74 23 560

26        Scopus Author iD: 6602163740

27

28 **Abstract**

29 According to the European statistics, approximately 26 million patients worldwide suffer  
30 from heart failure (HF), and this number seems to be steadily increasing. Inflammation plays  
31 a central role in the development of HF, and the pro-inflammatory cytokine Tumor necrosis  
32 factor- $\alpha$  (TNF- $\alpha$ ) represents inflammation gold-standard biomarker. Early detection plays a  
33 crucial role for the prognosis and treatment of HF. An Ion Sensitive Field Effect Transistor  
34 (ISFET) based on silicon nitride transducer and biofunctionalized with anti-TNF- $\alpha$  antibody  
35 for label-free detection of salivary TNF- $\alpha$  is proposed. Electrochemical impedance  
36 spectroscopy (EIS) was used for TNF- $\alpha$  detection. Our ImmunoFET offered a detection limit  
37 of  $1 \text{ pg mL}^{-1}$ , with an analytical reproducibility expressed by a coefficient of variance (CV)  
38 resulted  $< 10 \%$  for the analysis of saliva samples, and an analyte recovery of  $94 \pm 6 \%$ . In  
39 addition, it demonstrated high selectivity when compared to other HF biomarkers such as  
40 Interleukin-10, N-terminal pro B-type natriuretic peptide, and Cortisol. Finally, ImmunoFET  
41 accuracy in determining the unknown concentration of TNF- $\alpha$  was successfully tested in  
42 saliva samples by performing standard addition method. The proposed ImmunoFET showed  
43 great promise as a complementary tool for biomedical application for HF monitoring by a  
44 non-invasive, rapid and accurate assessment of TNF- $\alpha$ .

45

46

47 **Keywords**

48 Biosensor

49 ImmunoFET

50 Tumor necrosis factor- $\alpha$

51 Saliva analysis

52 Electrochemical impedance spectroscopy

53 Heart failure

## 54 **1. Introduction**

55 Heart failure (HF) is a complex clinical syndrome caused by a wide range of cardiovascular  
56 disorders, such as structural or functional abnormalities of the heart, which results in the  
57 impairment of the heart ability to fill or to pump out blood may eventually lead to the clinical  
58 syndrome of HF. This cardiovascular chronic disease is currently the main cause of mortality  
59 and poor quality of life in western societies, affecting approximately 26 million people  
60 worldwide, and its prevalence continues to rise over time, with aging of the population [1,2].  
61 Since HF imposes both direct costs to healthcare systems and indirect costs to society through  
62 morbidity, unpaid care costs, premature mortality and lost productivity, the estimation of  
63 global economic burden of HF is not accurately feasible. Therefore, increase of the population  
64 prone to HF requires a more specific and focused attention to both diagnosis and monitoring  
65 of the disease, both in the interest of patients than in the better management of costs linked to  
66 the spread of this disease [3,4]. In addition, patients with HF often present with signs and  
67 symptoms that are often nonspecific and with a wide differential diagnosis, making diagnosis  
68 by clinical presentation alone challenging that, unfortunately, can often result in delays in  
69 definitive diagnosis and treatment, and such delays are linked with poor prognosis [5].  
70 Therefore, additional tools to aid clinical assessment would result helpful in making an  
71 accurate and prompt diagnosis, and effectively prognosticate, treat and better identify high-  
72 risk subjects [6]. The detection of specific biomarkers, which are measurable biological  
73 markers of a pathological process, provides information about variety biological conditions  
74 whether normal or pathological, and they can also be exploited not only to diagnose HF, but  
75 also to monitor the course of the therapy [7]. Among the established HF biomarkers, a raised  
76 circulating level of several inflammatory cytokines has been observed due to systemic  
77 inflammation that characterizes HF patients [8–10]. In particular, Tumor necrosis factor-alpha  
78 (TNF- $\alpha$ ) is a pro-inflammatory cytokine observed following cardiac stress and whose  
79 dysregulation and excessive production were demonstrated implicated in the pathogenesis of  
80 HF as well as to adverse effects on other organs and apparatus, as well as on coagulation and  
81 immune system [11–13]. TNF- $\alpha$  is usually quantified in blood or plasma representing an  
82 additional stress, especially for elderly. Its concentration in healthy human plasma is usually  
83 less than 40 pg/mL [14,15], but its level increases up to hundreds according to HF severity  
84 [16,17]. TNF- $\alpha$  quantification is usually carried out in blood and by immunochemical  
85 methods, which provide accurate and provide rapid screening and multiple analyses, but  
86 several disadvantages also due to their high cost, the requirement of qualified personnel, and  
87 no possibility for real time measurement. For these reasons, biosensors are a very promising

88 alternative due to their easy to use, reduced cost, portability, and possibility of on-line  
89 monitoring of biomarkers by in-situ measurements [18–20]. At the same time, the  
90 concentration of TNF- $\alpha$  in serum is reflected by its salivary levels [21] making TNF- $\alpha$  an  
91 ideal salivary biomarker for HF monitoring. The interest to use saliva as target matrix is due  
92 to the several offers advantages offered by saliva analysis if compared to blood: an easier and  
93 unobtrusively sampling (even from critical subjects such as children, elder and disabled  
94 people), the suitability for the screening of a large population by passing several drawbacks  
95 such as invasiveness and psychological stress (especially if repeated sampling is needed), and  
96 less health risks for patients and healthcare professionals [15,22–25].  
97 In this paper we presented the development of an Ion Sensitive Field Effect Transistor  
98 (ISFET) based on silicon nitride transducer ( $\text{Si}_3\text{N}_4$ ) and biofunctionalized for TNF- $\alpha$   
99 detection in saliva for HF monitoring. For this purpose, monoclonal antibody TNF- $\alpha$  (mAb  
100 anti-TNF- $\alpha$ ) were addressed onto the  $\text{Si}_3\text{N}_4$  surface through covalent bonding of the aldehyde-  
101 silane (11-(triethoxysilyl) undecanal) TESUD obtaining an ImmunoFET. Our device provided  
102 a linear response and an adequate sensitivity for the target concentration range. Moreover,  
103 ImmunoFET selectivity was proven by analyzing samples containing three other HF  
104 biomarkers such as Interleukin-10 (IL-10), N-terminal pro B-type natriuretic peptide (NT-  
105 proBNP), and Cortisol. Matrix effect was also properly investigated. Finally, the developed  
106 ImmunoFET was used to quantify TNF- $\alpha$  in real saliva samples by performing the standard  
107 addition method (STAM). Satisfactory results, proven by a mean accuracy of 98%, confirmed  
108 that our ImmunoFET can represent a promising tool for TNF- $\alpha$  monitoring in saliva for HF  
109 monitoring. Even if some papers already report the development of electrochemical sensors or  
110 biosensors for salivary TNF- $\alpha$  detection [19,20,26], our device would offer an innovative and  
111 promising approach based on the first time use of ISFET as sensing transducer combined with  
112 electrochemical impedance spectroscopy (EIS) for saliva sample analysis.

113

## 114 **2. Materials and methods**

### 115 **2.1. Chemicals and reagents**

116 TNF- $\alpha$  (Cat. No. 210-TA), mAb anti-TNF- $\alpha$  (Cat. No. MAB610), IL-10 (Cat. No. 1064-IL),  
117 sterile phosphate buffer saline solution (PBS) and PBS containing 0.1% bovine serum  
118 albumin (Cat. No. RB01 and RB02, respectively) were from R&D Systems (BioTechne,  
119 France). Hydrocortisone (cortisol, purity 99%, Cat. No. ab141250) was from abcam (France).  
120 NT-proBNP (Cat. No. 8NT2) was from HyTest (Finland). Millipore Milli-Q nanopure water

121 (resistivity  $> 18 \text{ M}\Omega \text{ cm}$ ) was produced by a Millipore Reagent Water System (France). 11-  
122 triethoxysilyl undecanal (TESUD, 90%) was purchased from abcr (Germany). Pure ethanol  
123 (purity 95.0%) and sterile phosphate buffer saline (PBS) tablets were purchased from Sigma-  
124 Aldrich (France). PBS buffer used in this study was prepared by dissolving PBS tablets in the  
125 nanopure water as indicated by the supplier by yielding 0.01 M phosphate buffer (pH 7.4)  
126 containing 0.0027 M potassium chloride and 0.137 M sodium chloride. Epoxy resin EPO  
127 TEK H70E2LC was from Epoxy Technology (France).

128

## 129 **2.2. Instrumentation**

130 Wire bonding was performed using Kulicke & Soffa 4523 A Digital instrument from Kulicke  
131 & Soffa (Singapore). The UV/Ozone Procleaner™ (BioForce, Germany) was used in order to  
132 activate the ISFET's surface by creating  $-\text{OH}$  groups. The electrochemical measurements  
133 were performed using a VMP3 multichannel potentiostat purchased from Biologic-EC-Lab  
134 (France). Data acquisition and analysis were accomplished using EC-Lab software V11.30.

135

## 136 **2.3. ISFET bio-functionalization**

137 Microelectronic fabrication process for ISFET realization has been carried out at the National  
138 Microelectronics Centre (CSIC) of Institute of Microelectronics of Barcelona and it is  
139 described elsewhere [27]. ISFETs were bio-functionalized by the immobilization of mAb  
140 anti-TNF- $\alpha$  onto the ISFETs surface.

141 mAb anti-TNF- $\alpha$  have been diluted at  $0.5 \text{ mg mL}^{-1}$  in RB01 buffer according the procedure  
142 provided from the supplier. This stock solution was subsequently aliquoted and then stored at  
143  $-20 \text{ }^\circ\text{C}$  until use. The  $10 \text{ }\mu\text{g mL}^{-1}$  mAb anti-TNF- $\alpha$  standard solution needed for ISFET  
144 functionalization has been obtained by further dilution of mAb mother solution in RB01 after  
145 gentle defrosting at  $4 \text{ }^\circ\text{C}$  for 15 min before use.

146 The bio-functionalization process was started by cleaning the ISFETs with acetone/ethanol  
147 using sonicator bath; ISFETs were then thoroughly rinsed with Milli-Q water. Afterwards, the  
148 device was then placed for 30 min into the UV/O<sub>3</sub> cleaner to activate ISFET surface by  
149 creating  $-\text{OH}$  groups onto the  $\text{Si}_3\text{N}_4$  surface. Subsequently, the activated ISFETs were  
150 functionalized with TESUD ((11-triethoxysilyl) undecanal) using vapor-phase method, an  
151 activation process already presented by our group in which  $\text{Si}_3\text{N}_4$  and  $\text{HfO}_2$  surfaces have  
152 been aldehyde-functionalized to detect human serum albumin [28] and salivary cortisol [29],  
153 respectively

154 Then, the devices were placed into an oven at 100 °C for 1 h. After that, ISFETs were rinsed  
155 with absolute ethanol and dried using nitrogen to eliminate the excess of TESUD. Next, the  
156 functionalized ISFETs were incubated with mAb anti-TNF- $\alpha$  (10  $\mu\text{g mL}^{-1}$  in PBS). Finally,  
157 the ImmunoFET was left in ethanolamine (1% v/v in PBS) for 45 min at room temperature  
158 ( $20 \pm 2$  °C). This step was very important to prevent nonspecific bonding at the detection  
159 stage.

160

#### 161 **2.4. Standard solutions and saliva samples preparation**

162 TNF- $\alpha$  have been reconstituted at 0.1 mg mL $^{-1}$  in RB02 buffer according to the reconstitution  
163 procedure provided from the supplier. This stock solution was then aliquoted and stored at  
164  $-20$  °C until use. Before use, each aliquot (10  $\mu\text{L}$ ) was gently defrosted at 4 °C for 15 min and  
165 then it was further diluted in PBS to obtain working standard solutions needed for both  
166 calibrations in PBS (in the concentration range 1 – 50 pg mL $^{-1}$ ) and for spiking saliva  
167 samples.

168 Standard solutions containing other HF biomarkers in PBS (e.g. IL-10, NT-proBNP, and  
169 cortisol, in the concentration range 5 – 20 pg mL $^{-1}$ ) have been prepared in a similar way to  
170 carry out the interference study.

171 Saliva has been collected from nominally healthy volunteers according to a procedure  
172 described elsewhere [23,30]. Briefly, subjects were asked to freely roll a synthetic swab  
173 (Salivette<sup>®</sup> from Sarstedt, Germany) in their mouth. Saliva was then recovered by  
174 centrifugation of the swab at 7000 rpm for 5 min at 4 °C, and all samples were pooled. The  
175 pooled saliva sample (PSS) was then aliquoted.

176 One aliquot (5 mL) was used for preparing calibration samples (TNF- $\alpha$  calibration in saliva) to  
177 investigate both method linearity and matrix effect. Matrix effect was excluded by comparing,  
178 at a confidence level of 95%, the slopes, reported with the corresponding standard deviation, of  
179 the calibration curves obtained by analyzing TNF- $\alpha$  standard solutions in PBS and saliva  
180 samples spiked in the same concentration range [31].

181 Another aliquot (450  $\mu\text{L}$ ) was analyzed by performing the STAM. To confirm the result, two  
182 other aliquots (450  $\mu\text{L}$ ) were spiked with a known amount of TNF- $\alpha$  to obtain two samples  
183 containing 50 and 330 pg mL $^{-1}$  respectively. These samples have been treated as *unknown*  
184 *samples* and analyzed by carrying out the STAM.

185 STAM samples were prepared by adding a constant volume (50  $\mu\text{L}$ ) of sample to each of four  
186 1.5 mL Eppendorf<sup>®</sup> Lo-bind centrifuge tubes (Eppendorf, France). The first tube was then

187 made up to a final volume of 1 mL by adding 950  $\mu\text{L}$  of PBS, obtaining the sample  $C_0$ .  
188 Increasing volumes of a 500  $\text{ng mL}^{-1}$  TNF- $\alpha$  standard solution were added to the subsequent  
189 tubes and each flask was then made up to 1 mL with PBS, obtaining sample  $C_1$  (addition of 20  
190  $\text{pg mL}^{-1}$ ), sample  $C_2$  (addition of 50  $\text{pg mL}^{-1}$ ), and sample  $C_3$  (addition of 100  $\text{pg mL}^{-1}$ ),  
191 respectively. Afterwards, SAM samples were analyzed by EIS as described in 2.5.

192

## 193 **2.5. EIS measurements**

194 EIS measurements have been carried out after incubation at room temperature ( $20 \pm 2$   $^{\circ}\text{C}$ ) of  
195 the ImmunoFET in standard solutions, spiked saliva samples or STAM samples for 30 min  
196 each, followed by PBS washing. EIS measurements were carried out in PBS, with a frequency  
197 ranged from 10 KHz to 10 Hz, two frequency points per frequency decade, and using a  
198 modulation voltage of 75 mV ( $E_{ac}$ ). During the measurements, the potential was kept at 0 V  
199 ( $E_{dc}$ ) versus the Ag/AgCl reference. EIS measurements were performed at room temperature  
200 ( $20 \pm 2$   $^{\circ}\text{C}$ ) and in a faraday cage to avoid electrical and luminosity interference. The  
201 modeling of the obtained EIS data was achieved by the EC-Lab software using the  
202 Randomize + Simplex method, stopped on 5000 iterations.

203 Data fitting on EIS spectra was achieved using an equivalent circuit model [ $R_1 + Q_2/R_2$ ] shown  
204 in Fig. 1, in which  $R_1 = R_s$  and it corresponds to the resistance of the electrolyte solution (PBS);  
205  $Q_2$  is the constant phase element (CPE) that is in parallel with  $R_2$ , which is the charge transfer  
206 resistance ( $R_{ct}$ ). Curves were obtained by plotting the  $\Delta R/R$  normalized data as a function of  
207 TNF- $\alpha$  concentration.  $\Delta R/R$  values have been normalized using the following equation ( $R_{Ag} -$   
208  $R_{Ab})/R_{Ab}$ , where  $R_{Ag}$  corresponds to  $R_2$  of the antigen (TNF- $\alpha$ ), and  $R_{Ab}$  to the  $R_2$  of mAb anti-  
209 TNF- $\alpha$ .

210

211

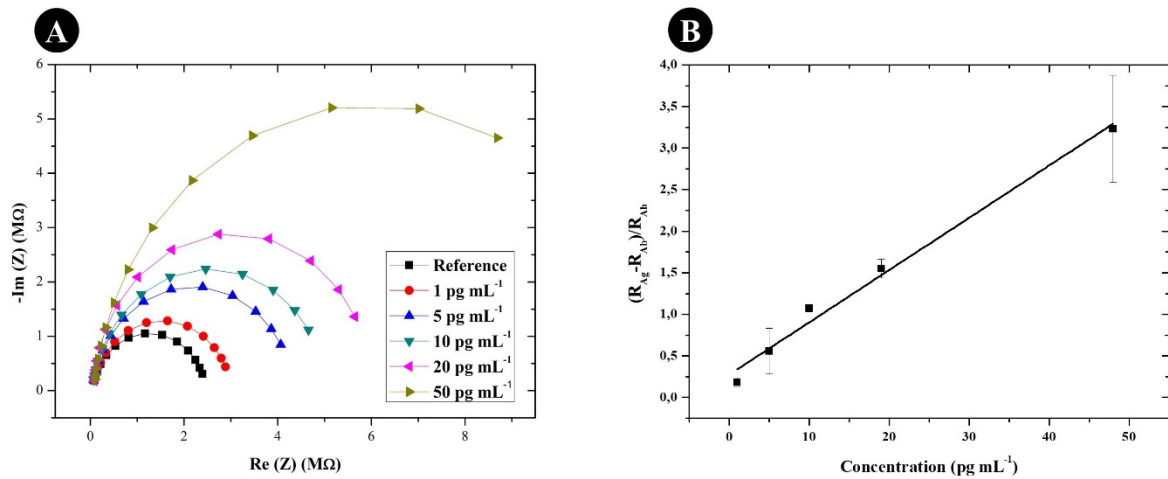
## 212 **3. Results and Discussion**

### 213 **3.1. Standard solution analysis**

214 Our ImmunoFET was first tested to verify the interaction between immobilized mAb anti-  
215 TNF- $\alpha$  and recombinant human TNF- $\alpha$  in the concentration range from 1 to 50  $\text{pg mL}^{-1}$ . This  
216 concentration range was chosen taking into account both the dilution factor of 20 provided for  
217 STAM sample preparation and the TNF- $\alpha$  concentration range expected in saliva collected  
218 from HF patients (from few dozen up to 1000  $\text{pg mL}^{-1}$ ). Fig .1A shows the Nyquist plots  
219 obtained by plotting the real part of impedance ( $\text{Re}(Z)$ ) against the imaginary part of  
220 impedance ( $-\text{Im}(Z)$ ). The  $R_{ct}$  increased accordingly to TNF- $\alpha$  concentration, confirming that



221 our developed ImmunoFET was sensitive to the raise of TNF- $\alpha$  concentration. The increase in  
 222  $R_{ct}$  is explained by the binding of TNF- $\alpha$  to the mAb anti-TNF- $\alpha$  immobilized onto the  
 223 ISFET, which produce an insulating layer that increases the  $R_{ct}$ . Then, the Nyquist plots  
 224 obtained were fitted using the equivalent circuit described in 2.5 and shown in Fig. 1A, and  
 225 the corresponding fitting parameters are presented in Table 1. Fig. 1B shows the related  
 226 calibration curve, confirming that our ImmunoFET response is linear to TNF- $\alpha$  concentration,  
 227 as demonstrated by  $R^2$  equal to  $0.988 \pm 0.027$  (CV% 2%). The calibration curve resulted  $y =$   
 228  $0.062 (\pm 0.011) x + 0.276 (\pm 0.011)$ . The limit of detection (LOD) of our ImmunoFET was  
 229 obtained from equation  $3 S/m$  [32], where  $S$  is the residual standard deviation of the linear  
 230 regression and  $m$  is the slope of the regression line, and resulted  $1 \text{ pg mL}^{-1}$ .  
 231



232  
 233 **Fig 1. (A)** Example of Nyquist plots for the equivalent circuit model obtained by analyzing TNF- $\alpha$   
 234 standard solutions in PBS (1; 5; 10; 20; and 50  $\text{pg mL}^{-1}$ ). EIS frequency ranged from 10 kHz to 10 Hz,  
 235 with  $E_{ac}$  75 mV and  $E_{dc}$  0 V vs Ag/AgCl; **(B)** Calibration curve obtained by analyzing standard  
 236 solution containing TNF- $\alpha$  in the concentration range 1 – 50  $\text{pg mL}^{-1}$  using the ImmunoFET  
 237 functionalized with mAb-TNF- $\alpha$ .  
 238  
 239  
 240

241 **Table 1.** Fitting parameters obtained from the equivalent circuit model  $[R_1 + Q_2/R_2]$ .  $R_1 = R_s$  is the resistance of  
 242 the electrolyte solution;  $Q_2$  is the constant phase element;  $R_2 = R_{ct}$  is the charge transfer resistance, and  $\chi$  is the  
 243 error on the fit.

Concentration	$R_1(\text{k}\Omega)$	$Q_2 (\text{nF}\cdot\text{s}^{(a-1)})$	$R_2 (\text{k}\Omega)$	$\chi$
Reference	33.270	1.339	2461	$7.318 \cdot 10^{-3}$
1 $\text{pg mL}^{-1}$	36.155	1.312	3004	$7.431 \cdot 10^{-3}$
5 $\text{pg mL}^{-1}$	39.539	1.098	4316	$5.731 \cdot 10^{-3}$
10 $\text{pg mL}^{-1}$	40.171	1.080	5032	$4.821 \cdot 10^{-3}$
20 $\text{pg mL}^{-1}$	43.680	1.058	6468	$6.216 \cdot 10^{-3}$
50 $\text{pg mL}^{-1}$	45.287	0.9759	11540	$3.371 \cdot 10^{-3}$

244

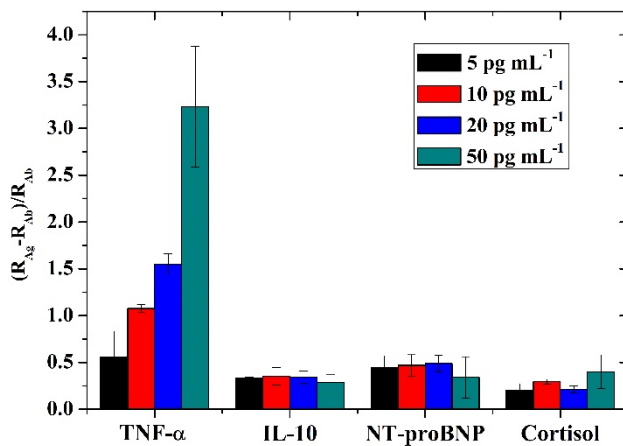
245

### 246 3.2. Selectivity study

247 Selectivity study was carried out by analyzing standard solutions containing TNF- $\alpha$  and three  
248 other HF biomarkers namely IL-10, NT-proBNP, and Cortisol in order to assess the levels of  
249 interferences from these biomarkers, using the same experimental conditions and concentration  
250 range from 5 to 50  $\text{pg mL}^{-1}$ . From Fig. 2, our ImmunoFET demonstrate to be highly selective  
251 toward TNF- $\alpha$  when compared to the other three HF biomarkers. In fact, the corresponding  
252 calibration curves resulted  $y = 0.060x + 0.372$  ( $R^2 = 0.993$ ) for TNF- $\alpha$ ;  $y = -0.001x + 0.357$  ( $R^2$   
253  $= 0.813$ ) for IL-10;  $y = -0.002x + 0.494$  ( $R^2 = 0.701$ ) for NT-proBNP; and  $y = 0.003x + 0.196$   
254 ( $R^2 = 0,708$ ) for cortisol.

255

256



257

258 **Fig 2.** Results from interference study obtained by analyzing standard solution containing TNF- $\alpha$  or  
259 other HF biomarkers (e.g. IL-10, NT-proBNP, and Cortisol) in the concentration range 5 – 50  $\text{pg}$   
260  $\text{mL}^{-1}$  using the ImmunoFET functionalized with mAb-TNF- $\alpha$ .

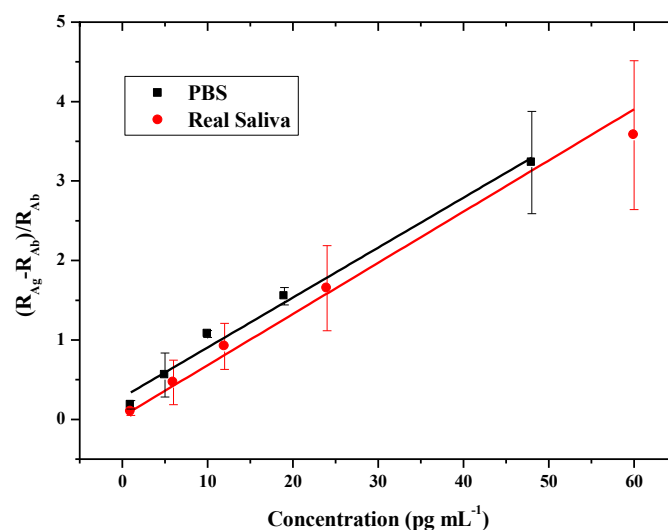
261

### 262 3.3. Saliva samples

#### 263 3.3.1. Calibration in saliva sample

264 Analysis of saliva calibration samples described in 2.4. provided a calibration curve described  
265 by  $y = 0.058 (\pm 0.014) + 0.144 (\pm 0.130)$  and confirmed the method linearity by an  $R^2$  equal  
266 to  $0.995 \pm 0.002$  (CV 0.2%). The presence of matrix effect was ruled out by comparing the  
267 slopes of the calibration curves (i.e. PBS and spiked saliva samples) at a confidence level of  
268 95%. The comparison of calibration curves in PBS and real saliva is shown in Fig. 3.

269



270  
 271 **Fig 3.** Comparison of calibration curves used for method linearity and matrix effect investigation that  
 272 were obtained from the analysis of TNF- $\alpha$  standard solution in PBS (black, described by  $y = 0.062 (\pm$   
 273  $0.011) x + 0.276 (\pm 0.011)$  with  $R^2 = 0.988 \pm 0.027$ ) and in spiked saliva samples (red, described by  $y =$   
 274  $0.058 (\pm 0.014) + 0.144 (\pm 0.130)$  with  $R^2 = 0.995 \pm 0.002$ ), respectively.

275  
 276  
 277

### 278 3.3.2. TNF- $\alpha$ quantification in saliva samples by STAM

279 TNF- $\alpha$  was then quantified in three aliquots of PSS (namely Aliquot I, II, and III,  
 280 respectively) by performing the standard addition method. As explained in 2.4, Aliquot I was  
 281 unspiked PSS, whereas Aliquot II and Aliquot III were PSS spiked with TNF- $\alpha$  standard  
 282 solution obtaining samples containing 50 and 330  $\text{pg mL}^{-1}$ , respectively.

283 The corresponding curves obtained from Aliquot I (which corresponded to unspiked PSS)  
 284 analysis by performing the STAM resulted linear and described by  $y = 0.076 (\pm 0.019) +$   
 285  $0.182 (\pm 0.053)$ , with  $R^2 = 0.998 (\pm 0.007)$ . According to STAM procedure, the concentration  
 286 of TNF- $\alpha$  in Aliquot I was extrapolated from the curve by multiplying for the dilution factor  
 287 of 20 the absolute value on x-axis for  $y = 0$ . In this case, TNF- $\alpha$  concentration in Aliquot I  
 288 resulted in  $48 \pm 12 \text{ pg mL}^{-1}$ . Aliquot II analysis provided a curve described by  $y = 0.013 (\pm$   
 289  $0.001) x + 0.059 (\pm 0.009)$  with  $R^2 = 0.995 (\pm 0.006)$  and TNF- $\alpha$  concentration resulted  $90 \pm$   
 290  $11 \text{ pg mL}^{-1}$ , whereas Aliquot III analysis provided a curve described by  $y = 0.013 (\pm 0.002) x$   
 291  $+ 0.253 (\pm 0.056)$ , with  $R^2 = 0.987 (\pm 0.007)$  and, consequently, TNF- $\alpha$  concentration resulted  
 292  $370 \pm 30 \text{ pg mL}^{-1}$ . Table 2 summarizes the results from analysis of STAM samples. Method  
 293 precision, here expressed as recovery %, was evaluated by considering the bias between the  
 294 expected TNF- $\alpha$  concentration and TNF- $\alpha$  calculated by extrapolation from the STAM curve,  
 295 and resulted  $94 \pm 6 \%$ .

296

297 **Table 2.** Data from saliva sample analysis by performing the STAM to quantify TNF- $\alpha$ .

Sample name	Sample type	Expected TNF- $\alpha$ concentration [pg mL <sup>-1</sup> ]	Calculated TNF- $\alpha$ concentration [pg mL <sup>-1</sup> ]
Aliquot I	Unspiked PSS	Unknown	48 $\pm$ 12 pg mL <sup>-1</sup>
Aliquot II	PSS spiked with 50 pg mL <sup>-1</sup>	TNF- $\alpha$ concentration in Aliquot I + 50 pg mL <sup>-1</sup>	90 $\pm$ 11 pg mL <sup>-1</sup>
Aliquot III	PSS spiked with 330 pg mL <sup>-1</sup>	TNF- $\alpha$ concentration in Aliquot I + 330 pg mL <sup>-1</sup>	370 $\pm$ 30 pg mL <sup>-1</sup>

298

299

300 These data (e.g. linearity, selectivity, high precision, and LOD of 1 pg mL<sup>-1</sup>) allowed to  
 301 consider our ImmunoFET as a very promising tool for monitoring salivary TNF- $\alpha$   
 302 concentration and further tests will be carried out and implemented to confirm these results  
 303 and carry out a pre-clinical study on HF patients.

304

305

#### 306 **4. Conclusions**

307 Preliminary results from ImmunoFET analytical validation (e.g. linearity, selectivity, high  
 308 precision, and LOD of 1 pg mL<sup>-1</sup>) allowed to consider our ImmunoFET as a very promising  
 309 tool for monitoring salivary TNF- $\alpha$  concentration. Our device also showed high selectivity  
 310 towards TNF- $\alpha$  when compared to other HF biomarkers such as IL-10, NT-proBNP, and  
 311 Cortisol. Finally, preliminary tests on TNF- $\alpha$  quantification saliva samples by performing the  
 312 STAM proved the capacity of our ImmunoFET to determine the TNF- $\alpha$  concentration with a  
 313 recovery almost quantitative, confirming the satisfying precision of the method. An  
 314 implementation of a clinical study would fully validate our device. In fact, these results,  
 315 combined with further improvements in term of accuracy and ImmunoFET integration into a  
 316 LoC, can allow the monitoring of salivary levels of TNF- $\alpha$  confirming our ImmunoFET as a  
 317 very promising tool for biomedical application such as HF monitoring by saliva analysis.

318

#### 319 **Acknowledgements**

320 The authors acknowledge the financial support of the European Union's Horizon 2020  
 321 research and innovation programme, Project NMBP-13-2017 KardiaTool (Grant agreement  
 322 No. 768686).

323

324 **Competing interests**

325 The authors declare no competing interests.

326

327

328 **References**

- 329 [1] E.J. Benjamin, P. Muntner, A. Alonso, M.S. Bittencourt, C.W. Callaway, A.P. Carson,  
330 A.M. Chamberlain, A.R. Chang, S. Cheng, S.R. Das, F.N. Delling, L. Djousse, M.S.V.  
331 Elkind, J.F. Ferguson, M. Fornage, L. Chaffin Jordan, S.S. Khan, B.M. Kissela, K.L.  
332 Knutson, T.W. Kwan, D.T. Lackland, T.T. Lewis, J.H. Lichtman, C.T. Longenecker, M.  
333 Shane Loop, P.L. Lutsey, S.S. Martin, K. Matsushita, A.E. Moran, M.E. Mussolino, M.  
334 O’Flaherty, A. Pandey, A.M. Perak, W.D. Rosamond, G.A. Roth, U.K.A. Sampson,  
335 G.M. Satou, E.B. Schroeder, S.H. Shah, N.L. Spartano, A. Stokes, D.L. Tirschwell,  
336 C.W. Tsao, M.P. Turakhia, L.B. VanWagner, J.T. Wilkins, S.S. Wong, S.S. Virani,;  
337 American Heart Association Council on Epidemiology and Prevention Statistics  
338 Committee and Stroke Statistics Subcommittee, Heart Disease and Stroke Statistics-  
339 2019 Update: A Report From the American Heart Association, *Circulation*. 139 (2019)  
340 e56–e528. <https://doi.org/10.1016/j.Sc.2010.00372>.
- 341 [2] S.S. Virani, A. Alonso, E.J. Benjamin, M.S. Bittencourt, C.W. Callaway, A.P. Carson,  
342 A.M. Chamberlain, A.R. Chang, S.Cheng, F.N. Delling, L. Djousse, M.S.V. Elkind, J.F.  
343 Ferguson, M. Fornage, S.S. Khan, B.M. Kissela, K.L. Knutson, T.W. Kwan, D.T.  
344 Lackland, T.T. Lewis, J.H. Lichtman, C.T. Longenecker, M. Shane Loop, P.L. Lutsey,  
345 S.S. Martin, K. Matsushita, A.E. Moran, M.E. Mussolino, A. Marma Perak, W.D.  
346 Rosamond, G.A. Roth, U.K.A. Sampson, G.M. Satou, E.B. Schroeder, S.H. Shah, C.M.  
347 Shay, N.L. Spartano, A. Stokes, D.L. Tirschwell, L.B. VanWagner, C.W. Tsao, and On  
348 behalf of the American Heart Association Council on Epidemiology and Prevention  
349 Statistics Committee and Stroke Statistics Subcommittee, Heart Disease and Stroke  
350 Statistics—2020 Update: A Report From the American Heart Association, *Circulation*.  
351 141 (2020) e139–e596. <https://doi.org/10.1161/CIR.0000000000000757>.
- 352 [3] W. Lesyuk, C. Kriza, P. Kolominsky-Rabas, Cost-of-illness studies in heart failure: a  
353 systematic review 2004–2016, *BMC Cardiovasc. Disord*. 18 (2018) 74.  
354 <https://doi.org/10.1186/s12872-018-0815-3>.
- 355 [4] A.A. Shafie, Y.P.Tan, C.H. Ng, Systematic review of economic burden of heart failure,  
356 *Heart. Fail. Rev*. 29 (2018) 131–145. <https://doi.org/10.1007/s10741-017-9661-0>.
- 357 [5] A.A. Inamdar, A.C. Inamdar, Heart Failure: Diagnosis, Management and Utilization, *J.*  
358 *Clin. Med*. 5 (2016) 62. <https://doi.org/10.3390/jcm5070062>.
- 359 [6] E.E. Tripoliti, T.G. Papadopoulos, G.S. Karanasiou, K.K. Naka, D.I. Fotiadis, Heart  
360 failure: Diagnosis, severity estimation and prediction of adverse events through machine  
361 learning techniques, *Comput. Struct. Biotechnol. J*. 15 (2016) 26–47.  
362 <https://doi.org/10.1016/j.csbj.2016.11.001>.
- 363 [7] E. Braunwald, Biomarkers in Heart Failure, *N Engl J Med*. 358 (2008) 2148–2159.  
364 <https://doi.org/10.1056/NEJMra0800239>.
- 365 [8] A. Yndestad, J.K. Damås, , E. Øie, E., T. Ueland, L. Gullestad, P. Aukrust, Role of  
366 inflammation in the progression of heart failure, *Curr. Cardiol. Rep*. 9 (2007) 236–241.  
367 <https://doi.org/10.1007/BF02938356>.
- 368 [9] L.F Shirazi, J. Bissett, F. Romeo, J.L. Mehta, Role of inflammation in heart failure,  
369 *Curr. Atheroscler. Rep*. 19 (2017) 27. <https://doi.org/10.1007/s11883-017-0660-3>.
- 370 [10] C. Riehle, J. Bauersachs, Key inflammatory mechanisms underlying heart failure, *Herz*.  
371 44 (2019) 96–106. <https://doi.org/10.1007/s00059-019-4785-8>.

- 372 [11] J. Holbrook, S. Lara-Reyna, H. Jarosz-Griffiths, M. McDermott, Tumour necrosis factor  
373 signalling in health and disease, *F1000Res.* 8 (2019) F1000 Faculty Rev-111.  
374 <https://doi.org/10.12688/f1000research.17023.1>
- 375 [12] M.J. Page, J. Bester, E. Pretorius, The inflammatory effects of TNF- $\alpha$  and complement  
376 component 3 on coagulation, *Sci. Rep.* 8 (2018) 1812. <https://doi.org/10.1038/s41598-018-20220-8>.
- 377 [13] L. Puimège, C. Libert, Van F. Hauwermeiren, Regulation and dysregulation of tumor  
378 necrosis factor receptor-1, *Cytokine Growth Factor Rev.* 25 (2014) 285–300.  
379 <https://doi.org/10.1016/j.cytogfr.2014.03.004>.
- 380 [14] G. Kleiner, A. Marcuzzi, V. Zanin, L. Monasta, G. Zauli, Cytokine Levels in the Serum  
381 of Healthy Subjects, *Mediators of Inflammation.* 2013 (2013) 1–6.  
382 <https://doi.org/10.1155/2013/434010>.
- 383 [15] F.G. Bellagambi, T. Lomonaco, P. Salvo, F. Vivaldi, M. Hangouët, S. Ghimenti, D.  
384 Biagini, F. Di Francesco, R. Fuoco, A. Errachid, Saliva sampling: Methods and devices.  
385 An overview, *TrAC* 124 (2020) 115781. <https://doi.org/10.1016/j.trac.2019.115781>.
- 386 [16] Schumacher SM, Naga Prasad SV. Tumor necrosis factor- $\alpha$  in heart failure: an updated  
387 review, *Curr. Cardiol. Rep.* 20 (2018) 117. <https://doi.org/10.1007/s11886-018-1067-7>.
- 388 [17] O.A. Segiet, A. Piecuch, L. Mielanczyk, M. Michalski, E. Nowalany-kozielska, Role of  
389 interleukins in heart failure with reduced ejection fraction, *Anatol. J. Cardiol.* 22 (2019)  
390 287–299. <https://doi.org/10.14744/AnatolJCardiol.2019.32748>.
- 391 [18] M. Lee, N. Zine, A. Baraket, M. Zabala, F. Campabadal, R. Caruso, M.G. Trivella, N.  
392 Jaffrezic-Renault, A. Errachid, A novel biosensor based on hafnium oxide: Application  
393 for early stage detection of human interleukin-10, *Sens. Actuator. B-Chem.* 175 (2012)  
394 201–207. <https://doi.org/10.1016/j.snb.2012.04.090>.
- 395 [19] L. Barhoumi, A. Baraket, F.G. Bellagambi, G.S. Karanasiou, M. Ben Ali, D.I. Fotiadis,  
396 J. Bausells, N. Zine, M. Sigaud, A. Errachid, A novel chronoamperometric  
397 immunosensor for rapid detection of TNF- $\alpha$  in human saliva, *Sens. Actuator. B-Chem.*  
398 266 (2018) 477–84. <https://doi.org/10.1016/j.snb.2018.03.135>.
- 399 [20] L. Barhoumi, A. Baraket, F.G. Bellagambi, F.M. Vivaldi, A. Baraket, Y. Clément, N.  
400 Zine, M. Ben Ali, A. Elaissari, A. Errachid, Ultrasensitive immunosensor array for  
401 TNF- $\alpha$  detection in artificial saliva using polymer-coated magnetic microparticles onto  
402 screen-printed gold electrode, *Sensors. (Basel).* 19 (2019) E692.  
403 <https://doi.org/10.3390/s19030692>.
- 404 [21] P. Gümüş, N. Nizam, D.F. Lappin, N. Buduneli, Saliva and Serum Levels of B-Cell  
405 Activating Factors and Tumor Necrosis Factor- $\alpha$  in Patients With Periodontitis, *Journal*  
406 *of Periodontology.* 85 (2014) 270–280. <https://doi.org/10.1902/jop.2013.130117>.
- 407 [22] A. Longo, A. Baraket, M. Vatteroni, N. Zine, J. Bausells, RogerFuoco, F. Di  
408 Francesco, G.S. Karanasiou, D.I. Fotiadis, A. Menciassi, A. Errachid, Highly sensitive  
409 electrochemical BioMEMS for TNF- $\alpha$  detection in human saliva: Heart Failure,  
410 *Procedia Eng.* 168 (2016) 97–100. <https://doi.org/10.1016/j.proeng.2016.11.156>.
- 411 [23] F.G. Bellagambi, I. Degano, S. Ghimenti, T. Lomonaco, V. Dini, M. Romanelli, F.  
412 Mastorci, A. Gemignani, P. Salvo, R. Fuoco, F. Di Francesco, Determination of salivary  
413  $\alpha$ -amylase and cortisol in psoriatic subjects undergoing the Trier Social Stress Test,  
414 *Microchem. Journal.* 136 (2018) 177–184.  
415 <https://doi.org/10.1016/j.microc.2017.04.033>.
- 416 [24] S. Ghimenti, T. Lomonaco, F.G. Bellagambi, D. Biagini, P. Salvo, M.G. Trivella, M.C.  
417 Scali, V. Barletta, M. Marzilli, F. Di Francesco, A. Errachid, R. Fuoco, Salivary lactate  
418 and 8-isoprostaglandin F<sub>2 $\alpha$</sub>  as potential non-invasive biomarkers for monitoring heart  
419 failure: a pilot study, *Sci. Rep.* 10 (2020) 7441. <https://doi.org/10.1038/s41598-020-64112-2>.
- 420  
421

- 422 [25] D. Biagini, T. Lomonaco, S. Ghimenti, J. Fusi, E. Cerri, F. De Angelis, F.G.  
423 Bellagambi, C. Oger, J.M. Galano, E. Bramanti, F. Franzoni, R. Fuoco, F. Di Francesco,  
424 Saliva as a non-invasive tool for monitoring oxidative stress in swimmers athletes  
425 performing a  $VO_{2max}$  cycle ergometer test, *Talanta*. 216 (2020) 120979.  
426 <https://doi.org/10.1016/j.talanta.2020.120979>.
- 427 [26] F.G. Bellagambi, A. Baraket, A. Longo, M. Vatteroni, N. Zine, J. Bausells, R. Fuoco, F.  
428 Di Francesco, P. Salvo, G.S. Karanasiou, D.I. Fotiadis, A. Menciassi, A. Errachid,  
429 Electrochemical biosensor platform for TNF- $\alpha$  cytokines detection in both artificial and  
430 human saliva: Heart failure, *Sens. Actuator. B-Chem.* 251 (2017) 1026–1033.  
431 <https://doi.org/10.1016/j.snb.2017.05.169>.
- 432 [27] D. Vozgirdaite, H. Ben Halima, F.G. Bellagambi, A. Alcacer, F. Palacio, N. Zine, J.  
433 Bausells, A., A. Errachid, Development of an ImmunoFET for the detection of TNF- $\alpha$   
434 in saliva: application to heart failure monitoring, submitted to *Appl. Mater. Interfaces*.
- 435 [28] D. Caballero, J. Samitier, J. Bausells, A. Errachid, Direct patterning of anti-human  
436 serum albumin antibodies on aldehyde-terminated silicon nitride surfaces for HSA  
437 protein detection, *Small*. 5 (2009) 1531–1534. <https://doi.org/10.1002/sml.200801735>.
- 438 [29] H.B. Halima, N. Zine, J. Gallardo-Gonzalez, A.E. Aissari, M. Sigaud, A. Alcacer, J.  
439 Bausells, A. Errachid, A novel cortisol biosensor based on the capacitive structure of  
440 hafnium oxide: Application for heart failure monitoring, in: 2019 20th International  
441 Conference on Solid-State Sensors, Actuators and Microsystems & Eurosensors  
442 XXXIII (TRANSDUCERS & EUROSENSORS XXXIII), IEEE, Berlin, Germany,  
443 2019: pp. 1067–1070. <https://doi.org/10.1109/TRANSDUCERS.2019.8808561>.
- 444 [30] T. Lomonaco, S. Ghimenti, D. Biagini, E. Bramanti, M. Onor, F.G. Bellagambi, R.  
445 Fuoco, F., Di Francesco, The effect of sampling procedures on the urate and lactate  
446 concentration in oral fluid, *Microchem. J.* 136 (2018) 255–262.  
447 <https://doi.org/10.1016/j.microc.2017.02.032>.
- 448 [31] D. Biagini, S. Antoni, T. Lomonaco, S. Ghimenti, P. Salvo, F.G. Bellagambi, R.T.  
449 Scaramuzza, M. Ciantelli, A. Cuttano, R. Fuoco, F. Di Francesco, F. Micro-extraction  
450 by packed sorbent combined with UHPLC-ESI-MS/MS for the determination of  
451 prostanoids and isoprostanoids in dried blood spots. *Talanta*. 206, 120236 (2020).  
452 <https://doi.org/10.1016/j.talanta.2019.120236>.
- 453 [32] A. Shrivastava, V. Gupta, Methods for the determination of limit of detection and limit  
454 of quantitation of the analytical methods, *Chron. Young. Sci.* 2 (2011) 21.  
455 <https://doi.org/10.4103/2229-5186.79345>.